Detecting Boundaries of Structural Differences in Long Time-span Image Samples for Remote Sensing Images and Medical Applications

Andrea Kovacs[1,2], Tamas Sziranyi[2]

[1] Pazmany Peter Catholic University, Faculty of Information Technology
kovan1@digitus.itk.ppke.hu
[2] Hungarian Academy of Sciences, Computer and Automation Research Institute
Distributed Events Analysis Research Group
sziranyi@sztaki.hu

Abstract. Finding structural changes in long time-span image samples is an important challenge: background may substantially change and saliency objects must be detected as the change of overall structure. The paper introduces novel methodologies to find salient changes against altering background. We will show that remote sensing and medical images have some common issues for similar tasks, and we also point at the differences. The proposed method finds changes in images scanned by a long time-interval difference in various lighting and radiometry conditions. The presented method is basically an exploitation of Harris saliency function and its derivatives for finding featuring points among image samples. To fit together the definition of keypoints and their active contour around them, we have introduced the Harris corner detection approach as an outline detector instead of the simple edge functions. Saliency points support the boundary hull definition of objects, constructing by graph based connectivity detection and neighborhood description. This graph based shape descriptor works on the saliency points of the difference and in-layer features. We prove the method in finding structural changes on remote sensing images.

1 Introduction

Long time-span diagnosis, surveillance or reconnaissance about the same area can be crucial for quick and up-to-date content retrieval. These tasks are usually suffer from the heavy changes in the background which make the simple differential or edge based methods unusable to detect structural developments.

In medical imaging, a continuous effort is given to find changes in MRI images. If the control scanning is frequently needed, the diagnosis must be done immediately. Therefore the huge amount of data and the comparison with database images urgently need automatic evaluation of such image series. Several methods have been implemented based on low-level vision and more complex methodologies, but usually they are specialized for a given problem: In [1] a nonlinear intensity normalization method is associated with statistical hypothesis test

methods to provide reliable change detection. In [2] MS lesions are treated as outliers to the normal brain tissue distribution, and the separation is achieved by minimizing a statistically robust L2E measure, which is defined as the squared difference between the true density and the assumed Gaussian mixture. In [3] the Alzheimer disease is detected by MR technique, where cortical changes do occur after central nervous system injury of different aetiology. In [4] to segment brain tissues in magnetic resonance images of the brain, they have implemented a stochastic relaxation method which utilizes partial volume analysis for every brain voxel with morphological processing and thresholding technique. In [5] a binary mask is generated and any lesion size found to be less than an input bound is eliminated from consideration.

Another important example is the automatic evaluation of aerial photographs, since manual administration of repositories is time consuming and cumbersome. The extraction of changes may facilitate applications like urban development analysis, disaster protection, agricultural monitoring and detection of illegal garbage heaps or wood cuttings. The obtained change map should provide useful information about size, shape or quantity of the changed areas, which could be applied directly by higher level object analyzer modules [6], [7]. The processing methods should consider that several optical image collections include partially archive data, where the photographs are grayscale or contain only poor color information. This paper focuses on finding contours of newly appearing/fading out objects in optical aerial images which were taken with several years time differences partially in different seasons and in altering lighting conditions. In this case, simple techniques like thresholding the difference image [8] or background modeling [9] cannot be adopted efficiently since details are not comparable.

These optical image sensors provide limited information and we can only assume to have image repositories which contain geometrically corrected and registered [10] grayscale orthophotographs.

In the literature one main group of approaches is the postclassification comparison, which segments the input images with different land-cover classes, like arboreous lands, barren lands and artificial structures [11], [12], obtaining the changes indirectly as regions with different classes in the two image layers [13]. We follow another methodology, like direct methods [14], [15], [15], [16], where a similarity-feature map from the input photographs is derived, then the feature map is separated into changed and unchanged areas.

Our direct method does not use any physical modeling (biophysical models or land-cover class models), and attempts to detect changes which can be discriminated by low-level features [17]. However, our approach is not a pixel-neighborhood MAP system as in [18], but a connection system of nearby saliency points. These saliency points define a connection system by using local graphs for outlining the local hull of the objects. Considering this curve as a starting spline, we search for objects' boundaries by active contour iterations.

The above features are local saliency points and saliency functions. The main saliency detector is calculated as a discriminative function among the functions of the different layers. We show that Harris detector is the appropriate function

for finding the dissimilarities among different layers, when comparison is not possible because of the different lighting, color and contrast conditions.

Local structure around keypoints is investigated by generating scale and position invariant descriptors, like SIFT. These descriptors describe the local microstructure, however, in several cases more succinct set of parameters is needed. For this reason we have developed a local active-contour based descriptor around keypoints, but this contour is generated by edginess in the cost function, while we characterize keypoints of junctions. To fit together the definition of keypoints and their active contour around them, we have introduced the Harris corner detection as an outline detector instead of the simple edge functions. This change resulted in a much better characterization of local structure.

In the following, we introduce a new change detection procedure by using Harris function and its derivatives for finding saliency points among image samples; then a new local descriptor will be demonstrated by generating local active contours. A graph based shape descriptor will be shown based on the saliency points of the difference and in-layer features. Finally, we prove the method's capabilities for finding structural changes on aerial and medical image series.

2 Change detection with Harris keypoints

2.1 Harris corner detector

The detector was introduced by Chris Harris and Mike Stephens in 1988 [19]. First, it computes the Harris matrix (M) for each pixel in the image. Then, instead of computing the eigenvalues of M, an R corner response is defined:

$$R = Det(M) - k * Tr^2(M) \tag{1}$$

This R characteristic function is used to detect corners. R is large and positive in corner regions and negative in edge regions. By searching for local maxima of a normalized R, the Harris keypoints can be found. R could also be used for edge detection: $|R|$ function is large and positive in corner and also positive but smaller in edge regions, and nearly zero in flat regions. We used this function in our later work. Figure 1 shows the result of Harris keypoint detection. On Figure 1(b) light regions shows the larger R values, so keypoints will be detected in these areas (Figure 1(c)).

2.2 Change detection

The advantage of Harris detector is its strong invariance to rotation and the R characteristic function's invariance to illumination variation and image noise. Therefore it could be used efficiently for change detection in airborne images. In these kind of images, changes can mean the appearance of new man-made objects, (like buildings or streets) or natural, environmental variations. As image pairs may be taken with large intervals of time, the area may change largely. In our case the pieces of the image pairs was taken in 2000 and 2005 (Figure 2).

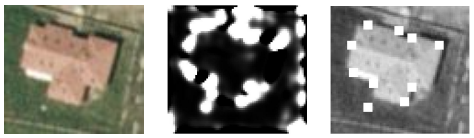

(a) Original (b) R function (c) Keypoints

Fig. 1. Operation of Harris detector: Corner points are chosen as the local maxima of the R characteristic function

(a) Older image (b) Newer image

Fig. 2. Original image pairs

It must be mentioned, that these image pairs are registered and represents exactly the same area. The registration process was performed by the Hungarian Institute of Geodesy, Cartography and Remote Sensing (FÖMI).

In our work we mainly focus on newly-born objects (buildings, pools or medical premonitory signatures). For airborne images, there are many difficulties when detecting such objects: the illumination and weather circumstances may vary, resulting different color, contrast and shadow conditions. The urban area might be imaged from different point of view. Buildings can be hidden by other structures, like trees, shadows, other buildings. These objects are quite various, which also makes the detection tough.

To overcome a part of the aforementioned difficulties, our idea was to use the difference of the image pairs. As we are searching for newly-built objects, we need to find buildups, that only exist on the newer image, therefore having large effect on the difference and the newer image. These areas can define the keypoint candidates, indicating newly built objects.

First, we examined the usability of intensity-based (Figure 3(a)) and edge-based difference map (Figure 3(b)).

Intensity-based and edge-based difference map is calculated as follows:

$$I_{\text{diff}}^{\text{int}} = |I_{\text{old}} - I_{\text{new}}| \tag{2}$$

$$I_{\text{diff}}^{\text{edge}} = |\text{edge}(I_{\text{old}}) - \text{edge}(I_{\text{new}})| \tag{3}$$

where I_{old} and I_{new} means the older and newer pieces of the image pairs respectively. We need grayscale images both for difference map generating, both

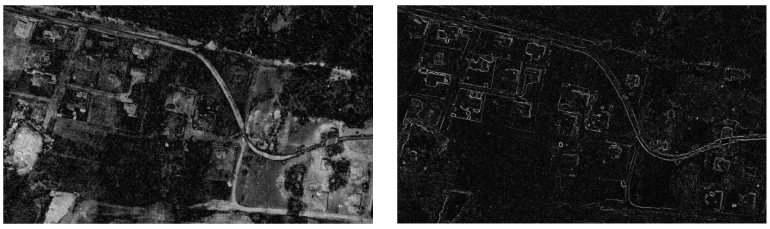

(a) Intensity-based difference map (b) Edge-based difference map

Fig. 3. Difference maps

for keypoint detection. According to our experiments, to enhance the change caused by buildups, it is more efficient to apply only the red component of the image (when talking about color images), rather than all the components. So, from now on, original images are meant as $I_{\text{old}} = I_{\text{old}}^{\text{red}}$ and $I_{\text{new}} = I_{\text{new}}^{\text{red}}$.

Moreover, the u^* component of the $L^*u^*v^*$ color space will also play an important role in our algorithm, as it enhances the red-coloured buildings and eliminates shadows.

The edge-based modification of I_{new} is also produced. $I_{\text{new}}^{\text{edge}} = \text{edge}(I_{\text{new}})$ (while $I_{\text{new}}^{\text{int}} = I_{\text{new}}$).

When searching for keypoint candidates, we call for Harris detector. As written before, the new objects have high effects both on the new and difference image, therefore we search for such keypoints that accomplish the next two criteria simultaneously:

1. $R(I_{\text{diff}}) > \epsilon_1$
2. $R(I_{\text{new}}) > \epsilon_2$

$R(...)$ indicates the Harris characteristic function (Eq. 1), ϵ_1 and ϵ_2 are thresholds. It is advised to take smaller ϵ_2, than ϵ_1. With this choice the difference map is preferred and has larger weight. Only important corners in the difference map will be marked.

Results of the keypoint detection is in Figure 4, detected keypoints are in white. As it can be seen, keypoints are mainly located around newly built buildings, but there are some false points (Figure 4(b)). Intensity-based detection has even poorer results, as in case of a few building, points are totally missing (Figure 4(a)). Intensity - and partially also edginess - is too sensitive to illumination change, so altering contrast and color conditions result the appearance of false edges and corner points and the vanishing of real ones in the difference map.

After analyzing the results, we decided to use another metric instead of intensity and edginess and redefine the difference map according to the new metric. The chosen metric was the normalized Harris R characteristic function ($\mathbf{R}$). Therefore the difference map was calculated as:

$$I_{\text{diff}}^{\text{R}} = |\mathbf{R}_{\text{old}} - \mathbf{R}_{\text{new}}| \tag{4}$$

(a) Intensity-based keypoints (b) Edge-based keypoints

Fig. 4. Detected keypoints

Modification of I_{new} looks as $I^{\text{R}}_{\text{new}} = \mathbf{R}_{\text{new}}$.

The difference map is in Figure 5(a).

The keypoint detection was the same as written before. Results are in Figure 5(b). Keypoints cover all buildings, and only a few points are in false areas.

After having some keypoint candidates indicating newly built objects, keypoints defining real changes should be selected somehow.

(a) R-based difference map (b) Keypoint detection

Fig. 5. Difference map and result of detection based on the R-function

3 Matching with Local Contours

3.1 Detection of similar structures

The local structure around keypoints should be an efficient description tool for comparison. Instead of using SIFT of high dimensionality, we have chosen a local contour descriptor, according to [20], as an efficient tool for describing the microstructure around Harris corner points. The main steps for estimating similar structure characteristics:

1. Generating Harris keypoints for difference map
2. Generating the Local Contour around keypoints in the image [21]

Fig. 6. Result of Local Contour matching with $|R|$-based edge map

3. Calculating Modified Fourier Descriptor for the estimated closed curve [22]
4. Describe the contour by a limited set of Fourier coefficients [23]
5. Comparing keypoints with a symmetric distance computation [23]

According to the last step, when comparing a keypoint (p_i) on the first frame and on the second frame, D_i represents the similarity value:

$$D_i(F_1, F_2, n) = \sigma(\frac{|F_{1,1}|}{|F_{2,1}|}, ..., \frac{|F_{1,n}|}{|F_{2,n}|}) + \sigma(\frac{|F_{2,1}|}{|F_{1,1}|}, ..., \frac{|F_{2,n}|}{|F_{1,n}|}) \tag{5}$$

where F_1 and F_2 denote the Modified Fourier Descriptors on the first and second frame, n is the number of Fourier coefficients applied (here $n = 20$).

If the following criteria exists:

$$D_i > \epsilon_3 \tag{6}$$

where $\epsilon_3 = 3$ is a tolerance value, than the keypoint is supposed to be a changed area.

After testing the algorithm, we realized that original active contours with intensity-based edge map are sensible to changes. Even for similar contours, the method often generated false positive result. This meant that changeless places were declared as newly built objects. Therefore we changed the external force of the original GVF snake with Harris normalized $|R|$ characteristic function (G_σ is the Gaussian function with σ standard deviation):

$$f_{|R|}(x, y) = G_\sigma(x, y) * |R(x, y)| \tag{7}$$

Result of the detection with the new edge map is provided in Figure 6.

3.2 Enhancing the number of saliency points with new characteristic function

After selecting the saliency points indicating change (P denotes the selected keypoint set), we have to enhance the number of keypoints. Therefore we are looking for saliency points which are not presented in the older image, but exists on the newer one. We apply the Harris corner detection method again with some modification.

Now not only corner points are essential, but also edge points of the objects, thus we need to modify the original Harris corner detector. In our case, when searching for both corners and edges, the eigenvalues can perform better. By denoting the eigenvalues of M (Harris matrix, see Section 2.1) by λ_1 and λ_2, we apply the following function instead of R:

$$R_{logmax} = max(0, log[max(\lambda_1, \lambda_2)]) \tag{8}$$

This metric has high values both in the edge and corner regions and low at the flat regions.

By calculating saliency points for older and newer image as well, an arbitrary $q_i = (x_i, y_i)$ point is selected if it satisfies all of the following conditions:
(1.) $q_i \in S_{logmax,\text{new}}$
(2.) $q_i \notin S_{logmax,\text{old}}$
(3.) $d(q_i, p_j) < \epsilon_4$
$S_{logmax,\text{new}}$ and $S_{logmax,\text{old}}$ are the sets of keypoints generated in the newer and older image, $d(q_i, p_j)$ is the Euclidean distance of q_i and p_j, where p_j denotes the point with smallest Euclidean-distance to q_i selected from the set $P \cup S_{logmax,\text{old}}$.

New points are searched iteratively, with $\epsilon_4 = 10$ condition. Here, ϵ_4 depends on the resolution of the image and on the size of buildings. If resolution is smaller, than ϵ_4 has to be chosen as a smaller value.

Figure 7 shows the enhanced number of keypoints.

3.3 Reconciling edge detection and corner detection

Now an enhanced set of saliency points is given, denoting possible area of changes, which can be the basis of building detection. We redefine the problem in terms of graph theory. [24]

A graph G is represented as $G = (V, E)$, where V is the vertex set, E is the edge network. In our case, V is already defined by the enhanced set of Harris points. Therefore, E needs to be formed.

Information about how to link the vertices can be gained from edge maps. These maps can help us to only match vertices belonging to the same building.

If objects have sharp edges, we need such image modulations, which emphasize these edges as far as it is possible. We have already written that R component of RGB and u^* component of $L^*u^*v^*$ color space can intensify grayish and redish object contours. Both of them operates suitably, therefore we apply both.

Fig. 7. Enhanced number of Harris keypoints

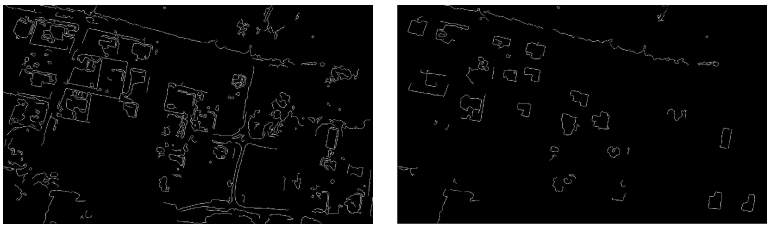

(a) Edge detection on R component (b) Edge detection on u^* component

Fig. 8. Result of Canny edge detection on different color components

By generating the R and u^* components (further on denoted as $I_{\text{new},r}$ and $I_{\text{new},u}$) of the original, newer image, Canny edge detection [25] with large threshold ($Thr = 0.4$) is executed on them. $C_{\text{new},r}$ and $C_{\text{new},u}$ marks the result of Canny detection. (Figure 8(a) and 8(b))

The process of matching is as follows. Given two vertices: $v_i = (x_i, y_i)$ and $v_j = (x_j, y_j)$. We match them if they satisfy the following conditions:
(1.) $d(v_i, v_j) = \sqrt{(x_j - x_i)^2 + (y_j - y_i)^2} < \epsilon_5$,
(2.) $C_{\text{new},\ldots}(x_i, y_i) = 1$,
(3.) $C_{\text{new},\ldots}(x_j, y_j) = 1$,
(4.) $\exists$ a finite path between v_i and v_j.
$C_{\text{new},\ldots}$ indicates either $C_{\text{new},r}$ or $C_{\text{new},u}$. ϵ_5 is a tolerance value, which depends on the resolution and average size of the objects. We apply $\epsilon_5 = 30$.

These conditions guarantee that only vertices connected in the edge map are matched.

Fig. 9. Subgraphs given after matching procedure

We obtain a graph composed of many separate subgraphs, which can be seen in Figure 9. Each of these connected subgraph is supposed to represent a building. However, there might be some unmatched keypoints, indicating noise. To discard them, we select subgraphs having at least two vertices.

To determine the contour of the subgraph-represented buildings, we used the aforementioned GVF snake method. The convex hull of the vertices in the subgraphs is applied as the initial contour.

4 Experiments and evaluation

Some results of the contour detection can be seen in Figure 10. Images were generated based on the u^* component.

The main advantage of our method is that it does not need any building template and can detect objects of any size and shape. The method has difficulties in finding objects with similar color to the background and sometimes one object is described with more than one subgraphs (like on the right end of the second row). These problems need to be solved in a forthcoming semantic or object evaluation step.

The algorithm was also evaluated on long time-span medical images. Registered MRI images of a patient scanned with long time-interval were examined, searching for MS-lesions.

Some changes need to be performed as we are searching for different objects and the images are also different.

MRI scans are grayscale images, therefore the conversion to $L^*u^*v^*$ color space is unnecessary, we only need the original image itself.

In case of these images, we are searching for circle-like shapes, not objects with sharp corners. For this reason, in the first step of the algorithm (Section

Fig. 10. Results of the contour detection

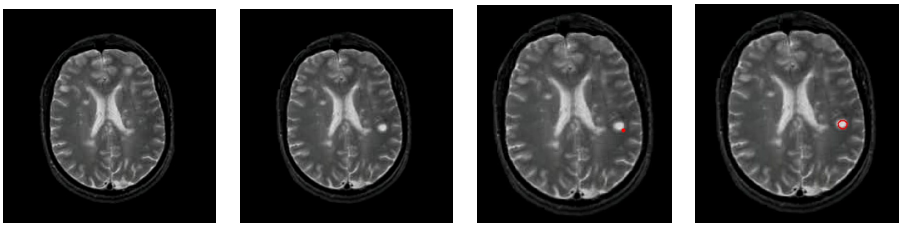

Fig. 11. Result of lesion detection with different maps: (a): Older image, (b): Newer image with lesion, (c): Intensity-based detection, (d): Harris-based detection

2.2) keypoint candidates were searched with the R_{logmax} function (Section 3.2) instead of the original R. Intensity-based saliency point detection must also be considered when working on grayscale images.

As lesions are the most salient on the difference map, there is no need to apply the Local Contour matching step (written in Section 3.1).

Result of lesion detection can be seen in Figure 11.

Acknowledgements

The authors would like to thank for the registered image pairs to Hungarian Institute of Geodesy, Cartography and Remote Sensing (FÖMI).

References

1. Bosc, M., Heitz, F., Armspach, J., Namer, I., Gounot, D., Rumbach, L.: Automatic change detection in multimodal serial mri: application to multiple sclerosis lesion evolution. NeuroImage **20** (2003) 643–656

2. Liu, J., Smith, C., Chebrolu, H.: Automatic multiple sclerosis detection based on integrated square estimation. In: IEEE. (2009) 31–38
3. Rocca, M., Filippi, M.: Functional mri to study brain plasticity in clinical neurology. Neurol Sci **27** (2006) S24–S26
4. Johnston, B., Atkins, M.S., Mackiewich, B., Anderson, M.: Segmentation of multide sclerosis lesions in intensity corrected multispectral mri. IEEE Tr. Medical Images **15** (1996) 154–169
5. Boudraa, A., Dehak, S., Zhub, Y., Pachaib, C., Baob, Y., Grimaud, J.: Automated segmentation of multiple sclerosis lesions in multispectral mr imaging using fuzzy clustering. Computers in Biology and Medicine **30** (2000) 23–40
6. Peng, T., Jermyn, I.H., Prinet, V., Zerubia, J.: Incorporating generic and specific prior knowledge in a multi-scale phase field model for road extraction from vhr images. IEEE Trans. Geoscience and Remote Sensing **1** (2008) 139–146
7. Lafarge, F., Descombes, X., Zerubia, J., Pierrot Deseilligny, M.: Automatic building extraction from dems using an object approach and application to the 3d-city modeling. **63** (2008) 365–381
8. Benedek, C., Szirányi, T., Kato, Z., Zerubia, J.: Detection of object motion regions in aerial image pairs with a multilayer markovian model. Trans. Img. Proc. **18** (2009) 2303–2315
9. Benedek, C., Szirányi, T.: Bayesian foreground and shadow detection in uncertain frame rate surveillance videos. **17** (2008) 608–621
10. Shah, C., Sheng, Y., Smith, L.: Automated image registration based on pseudoinvariant metrics of dynamic land-surface features. Geoscience and Remote Sensing **46** (2008) 3908–3916
11. Castellana, L., d'Addabbo, A., Pasquariello, G.: A composed supervised/unsupervised approach to improve change detection from remote sensing. Pattern Recognition Letters **28** (2007) 405–413
12. Benedek, C., Descombes, X., Zerubia, J.: Building extraction and change detection in multitemporal remotely sensed images with multiple birth and death dynamics. In: IEEE Workshop on Applications of Computer Vision (WACV), Snowbird, USA (2009) 100–105
13. Zhong, P., Wang, R.: A multiple conditional random fields ensemble model for urban area detection in remote sensing optical images. **45** (2007) 3978–3988
14. Ghosh, S., Bruzzone, L., Patra, S., Bovolo, F., Ghosh, A.: A context-sensitive technique for unsupervised change detection based on hopfield-type neural networks. **45** (2007) 778–789
15. Wiemker, R.: An iterative spectral-spatial bayesian labeling approach for unsupervised robust change detection on remotely sensed multispectral imagery. (1997) 263–270
16. Bazi, Y., Bruzzone, L., Melgani, F.: An unsupervised approach based on the generalized gaussian model to automatic change detection in multitemporal sar images. **43** (2005) 874–887
17. Kovacs, A., Sziranyi, T.: New saliency point detection and evaluation methods for finding structural differences in remote sensing images of long time-span samples. In: Proceedings of Conference on Advanced Concepts for Intelligent Vision Systems, Part II, Sydney, Australia (2010) 272–283
18. Benedek, C., Szirányi, T.: Change detection in optical aerial images by a multi-layer conditional mixed markov model. IEEE Trans. Geoscience and Remote Sensing **47** (2009) 3416–3430

19. Harris, C., Stephens, M.: A combined corner and edge detector. In: Proceedings of the 4th Alvey VisionConference. (1988) 147–151
20. Kovacs, A., Sziranyi, T.: Local contour descriptors around scale-invariant keypoints. In: Inernational Conference on Image Processing, Cairo, Egypt (2009) 1105–1108
21. Xu, C., Prince, J.L.: Gradient vector flow: A new external force for snakes. In: IEEE CVPR. (1997) 66–71
22. Rui, Y., She, A., Huang, T.: A modified fourier descriptor for shape matching in MARS. In: Image Databases and Multimedia Search. (1998) 165180
23. Licsar, A., Sziranyi, T.: User-adaptive hand gesture recognition system with interactive training. Image and Vision Computing, **23** (2005) 1102–1114
24. Sirmacek, B., Unsalan, C.: Urban-area and building detection using sift keypoints and graph theory. IEEE Trans. Geoscience and Remote Sensing **47** (2009) 1156–1167
25. Canny, J.: A computational approach to edge detection. IEEE Trans. Pattern Analysis and Machine Intelligence **8** (1986) 679–698